

DOI: 10.1002/cbic.201200728

The Interaction of Isopenicillin N Synthase with Homologated Substrate Analogues δ -(L- α -Amino adipoyl)-L-homocysteinyl-D-Xaa Characterised by Protein Crystallography

Adam Daruzzaman,^[a] Ian J. Clifton,^[a] Robert M. Adlington,^[a] Jack E. Baldwin,^{*,[a]} and Peter J. Rutledge^{*,[b]}

Isopenicillin N synthase (IPNS) converts the linear tripeptide δ -(L- α -amino adipoyl)-L-cysteinyl-D-valine (ACV) into bicyclic isopenicillin N (IPN) in the central step in the biosynthesis of penicillin and cephalosporin antibiotics. Solution-phase incubation experiments have shown that IPNS turns over analogues with a diverse range of side chains in the third (valinyl) position of the substrate, but copes less well with changes in the second (cysteinyl) residue. IPNS thus converts the homologated tripeptides δ -(L- α -amino adipoyl)-L-homocysteinyl-D-valine (AhCV) and δ -(L- α -amino adipoyl)-L-homocysteinyl-D-allylglycine (AhCaG) into monocyclic hydroxy-lactam products; this suggests that the additional methylene unit in these substrates induces conformational changes that preclude second ring closure after initial lactam formation. To investigate this and solu-

tion-phase results with other tripeptides δ -(L- α -amino adipoyl)-L-homocysteinyl-D-Xaa, we have crystallised AhCV and δ -(L- α -amino adipoyl)-L-homocysteinyl-D-S-methylcysteine (AhCmC) with IPNS and solved crystal structures for the resulting complexes. The IPNS:Fe^{II}:AhCV complex shows diffuse electron density for several regions of the substrate, revealing considerable conformational freedom within the active site. The substrate is more clearly resolved in the IPNS:Fe^{II}:AhCmC complex, by virtue of thioether coordination to iron. AhCmC occupies two distinct conformations, both distorted relative to the natural substrate ACV, in order to accommodate the extra methylene group in the second residue. Attempts to turn these substrates over within crystalline IPNS using hyperbaric oxygenation give rise to product mixtures.

Introduction

Isopenicillin N synthase (IPNS) is a non-heme iron enzyme that catalyses conversion of δ -(L- α -amino adipoyl)-L-cysteinyl-D-valine (ACV, **1**, Scheme 1) into isopenicillin N (IPN, **2**).^[1] This enzyme and its reaction behaviour have been studied extensively, in a wide range of spectroscopic,^[2–4] mechanistic,^[1,5] theoretical^[6,7] and crystallographic experiments.^[8–10] It is generally agreed that IPNS catalysis proceeds via high-valent iron-oxo intermediate **3**.^[10,11]

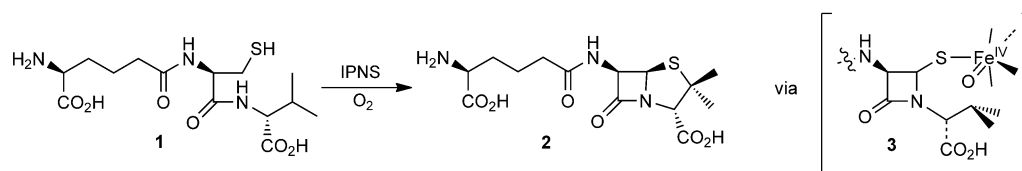
Of the many and various analogues of ACV (**1**) to have been subjected to reaction with IPNS,^[5] substrates in which the second residue (L-cysteine) is replaced by L-homocysteine revealed a particularly rich vein of unexpected oxidative chemistry.^[12–14] The reaction of δ -(L- α -amino adipoyl)-L-homocysteinyl-D-valine (AhCV, **4**, Scheme 2) was first studied to probe the substrate specificity of IPNS with regard to the central residue of its substrate, and in the hope of shedding light on the then

putative monocyclic intermediate **3**.^[12] Incubation of **4** with IPNS yielded the epimeric γ -lactam alcohols **5** (Scheme 2), which were shown to epimerise in aqueous solution at pH 7.5. The corresponding reaction with δ -(L- α -amino adipoyl)-L-homocysteinyl-D-allylglycine (AhCaG) gave an analogous γ -lactam alcohol product.^[12]

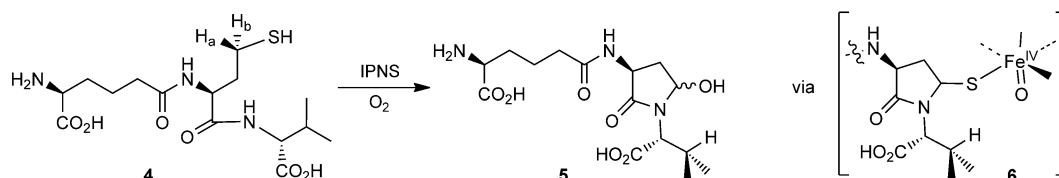
Repeating the reaction of **4** with IPNS under ¹⁸O₂ revealed significant ¹⁸O incorporation into the hydroxy group of the product **5** (although levels of incorporation were lower than seen with other hydroxylated products of IPNS incubations, presumably because the 5-OH is readily exchanged via an acyl iminium ion intermediate). Incubation of monodeuterated peptides in which either H_a or H_b is stereospecifically replaced by D gave the partially 5-deuterated γ -lactam; levels of deuterium loss were consistent with a degree of stereospecificity akin to that observed during conversion of ACV (**1**) into IPN (**2**): “ca. 80% of the maximum theoretical deuterium loss expected for a fully stereospecific event at the 4-position of the homocysteinyl residue” was observed with the deuterated analogues of **4**.^[12] A mechanism was proposed for formation of **5**, through initial formation of the monocyclic γ -lactam **6**, homologue of the ACV-derived β -lactam **3**. However, it seems that the iron(IV)-oxo unit in **6** cannot execute hydrogen abstraction from the valinyl β -carbon, for steric and/or stereoelectronic reasons. Instead, the high-valent intermediate is quenched by

[a] Dr. A. Daruzzaman, Dr. I. J. Clifton, Dr. R. M. Adlington, Prof. Sir J. E. Baldwin
Chemistry Research Laboratory, University of Oxford
Mansfield Rd, Oxford, OX1 3TA (UK)
E-mail: jack.baldwin@chem.ox.ac.uk

[b] Dr. P. J. Rutledge
School of Chemistry F11, The University of Sydney
Sydney, NSW 2006 (Australia)
E-mail: peter.rutledge@sydney.edu.au



Scheme 1. IPNS converts the linear tripeptide ACV (**1**) into bicyclic IPN (**2**); the reaction is generally agreed to proceed via the monocyclic β -lactam intermediate **3**.



Scheme 2. The reaction of AhCV (**4**) with IPNS gave the hydroxy γ -lactam **5**, presumably via monocyclic intermediate **6**.

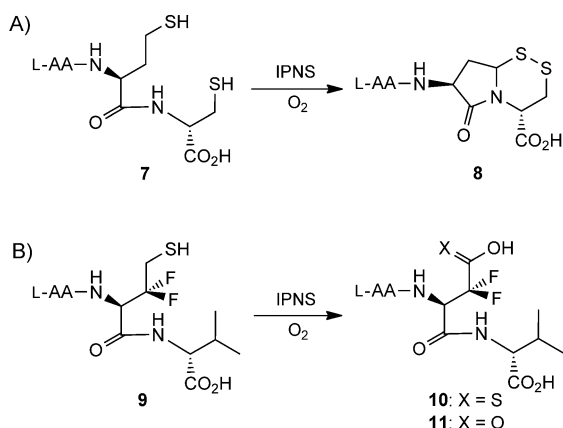
other means, leaving the enzyme-bound γ -lactam to collapse to an acyl iminium ion, which is hydrolysed to the observed product **5**. The alternative means of iron(IV)-oxo quenching and the end fate of the sulfur atom were not resolved.

Attempts to answer these questions with further incubation experiments raised more questions. δ -(L- α -Amino adipoyl)-L-homocysteinyl-D-cysteine (**7**) was converted into the bicyclic γ -lactam disulfide **8** by IPNS (Scheme 3A); this suggests Fe–S

conditions), suggesting that **10** is the sole product of the enzymatic reaction.

Crystallography has significantly enhanced our understanding of IPNS catalysis.^[8–10,15] Crystal structures of IPNS with its natural substrate and analogues have elucidated different modes of substrate and analogue binding, and revealed the influence of active site geometry on reactivity.^[9,16–21] The application of hyperbaric oxygenation to trigger reaction within crystalline IPNS has rendered further detail, allowing the enzyme mechanism to be studied step-by-step within the crystalline protein.^[10,22–26]

Here we report the results of a crystallographic investigation into the reaction of IPNS with AhCV (**4**). Using protein crystallography we have characterised the binding of AhCV (**4**) and methylsulfide analogue δ -(L- α -amino adipoyl)-L-homocysteinyl-D-S-methylcysteine (AhCmC, **12**, Scheme 4) to IPNS.



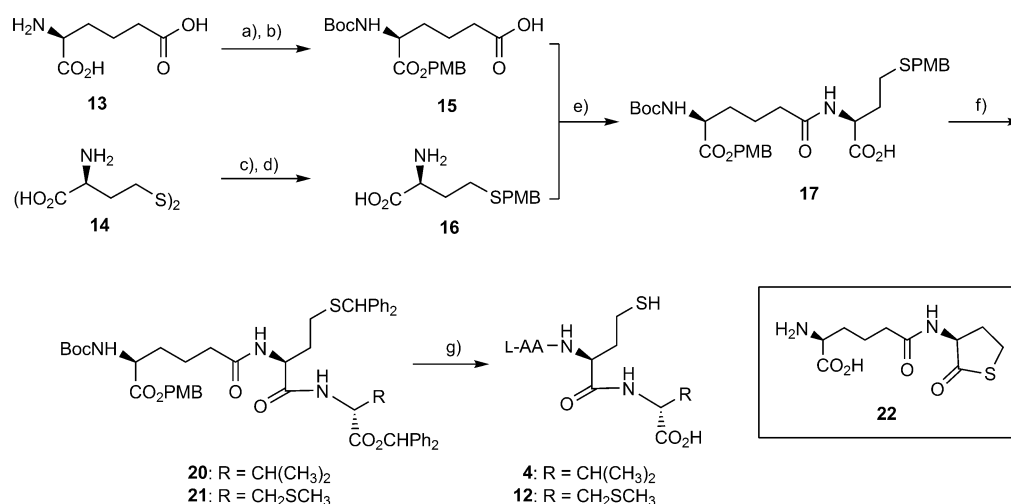
Scheme 3. IPNS converts: A) AhCC (**7**) into bicyclic disulfide **8**, and B) fluorinated analogue **9** into thiocarboxylate **10** and carboxylate **11** products. L-AA = δ -(L- α -amino adipoyl).

bond cleavage by the terminal cysteine thiolate group in an intermediate akin to **6**.^[13] The fluorinated analogue δ -(L- α -amino adipoyl)-L-3,3-difluorohomocysteinyl-D-valine (**9**) was designed to stabilise the enzyme-bound intermediate corresponding to **6** and prevent iminium ion formation; incubation of **9** with IPNS gave thiocarboxylic acid **10** and carboxylic acid **11** in a ratio of >5:1.^[14] The purified thiocarboxylate **10** was shown to decompose to carboxylate **11** at pH 7.5 (IPNS incubation

Results and Discussion

Synthesis of tripeptides

AhCV (**4**) and AhCmC (**12**) were prepared from the constituent amino acids L- α -amino adipic acid (**13**), L-homocystine (**14**) and D-valine or D-S-methylcysteine (Scheme 4). L- α -Amino adipic acid (**13**) was converted into the doubly-protected derivative **15** in good yield (55% over two steps) as previously reported.^[23] The disulfide **14** was reductively cleaved with sodium and liquid ammonia by the du Vigneaud procedure^[27] and protected in situ to give the PMB thioether **16** in high yield (83% over two steps). Isobutyl chloroformate-mediated coupling of acid **15** and amine **16** gave dipeptide **17** in excellent yield (90%). D-Valine and D-S-methylcysteine (obtained from D-cystine as reported by du Vigneaud)^[27] were converted into the corresponding benzhydryl esters **18** and **19**, respectively,^[28] and were then coupled to dipeptide **17** by diimide methodology to afford the fully protected tripeptides **20** and **21**. Global deprotection with TFA^[29] gave AhCV (**4**) or AhCmC (**12**) as their TFA salts, from which the pure tripeptides were



Scheme 4. Synthesis of tripeptide analogues **4** and **12**; a) NaOH, (Boc)₂O, H₂O/*t*BuOH, RT, 92%; b) PMBCl, Et₃N, DMF, 38 °C, 60%; c) Na, NH₃(l), -78 °C; d) PMBCl, -78 °C to RT, 83% (over two steps); e) isobutyl chloroformate, Et₃N, THF/H₂O, 0 °C, 90%; f) **18** or **19**, EDCI, HOBT, Et₃N, CH₂Cl₂, RT, 66% (**20**)/46% (**21**); g) TFA, anisole, reflux, RP-HPLC 46% (**4**)/12% (**12**); L-AA = δ-(L-α-amino adipoyl). Insert: the cyclic thioester **22** was isolated as the major product from TFA-mediated deprotection of **21**.^[21]

obtained by reversed-phase HPLC. Deprotection of the *S*-methylcysteine derivative **21** also gave rise to a significant quantity of the cyclic thioester **22**,^[21] which is presumably formed through thiol-mediated cleavage of the amide bond under the acidic conditions of the deprotection reaction.

The structure of the IPNS:Fe^{II}:AhCV complex

The crystal structure of the IPNS:Fe^{II}:AhCV complex was solved to 1.40 Å resolution (Figure 1, Table 1). The structure of the protein is generally well defined, and closely mirrors the structures of other IPNS:Fe^{II}:substrate analogue complexes.^[9,16–18,30,31] The active site iron is bound by the familiar triad of protein side chains (His214, Asp216 and His270), a water ligand opposite His214 and the homocysteiny l thiolate group opposite His270. The substrate AhCV (**4**) is less well de-

efined. Regions of the tripeptide that are tethered to the protein—the amino adipoyl amino and α-carboxylate groups, the homocysteiny l thiolate group and the valinyl carboxylate group—are clearly resolved. However the electron density defining other parts of the substrate is less clear, evincing conformational freedom and multiple occupancy in these regions (which include the amino adipoyl γ-, δ- and ε-centres, the homocysteiny l N, carbonyl, α-, β- and γ-carbons, and the valinyl Cα and side chain). There is also evidence for partial occupancy by a second water ligand at iron, in the binding site *trans* to Asp216.

It appears that AhCV (**4**) occupies the IPNS active site as a mixture of several conformers, but that two of these predominate; these are discussed as conformations A and B in more detail below. Conformation A is a skeletal arrangement close to that observed for the natural substrate ACV (**1**):^[9] iron

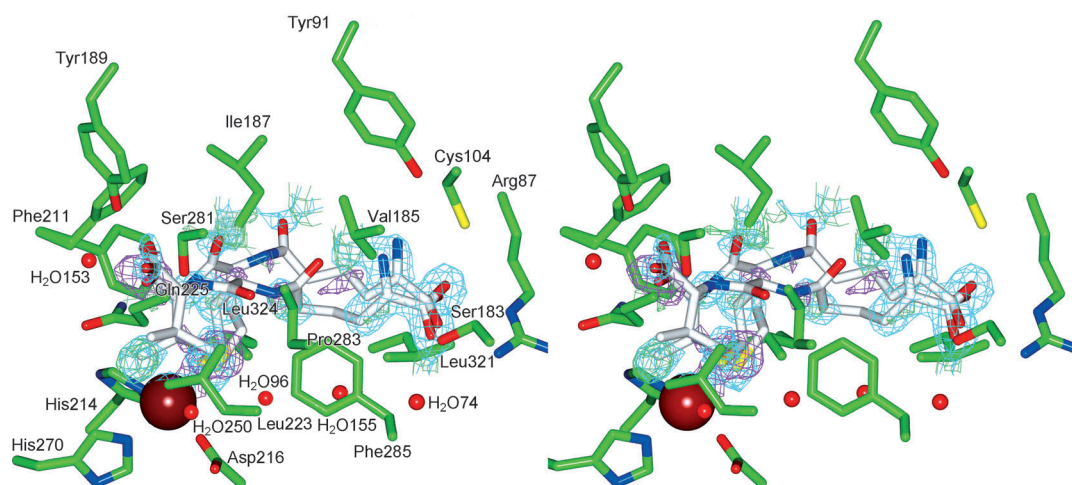


Figure 1. Stereoview of the active site of the IPNS:Fe^{II}:AhCV complex, showing electron density as: $2mF_o - Dfc$ density^[43] at 1σ (cyan) and $mF_o - Dfc$ density at $\pm 3\sigma$ [green ($+3\sigma$) and magenta (-3σ)], where σ is the RMS value of each map over an asymmetric unit. The figure was generated using CCP4mg.^[44]

Table 1. Crystallographic data for IPNS:Fe^{II}:AhCV and IPNS:Fe^{II}:AhCmC

	IPNS:Fe ^{II} :AhCV	IPNS:Fe ^{II} :AhCmC
X-ray source	ESRF beamline ID14EH2	ESRF beamline ID14EH1
wavelength [Å]	0.933	0.934
PDB ID	3zku	3zky
resolution [Å]	1.40	1.45
space group	P2 ₁ 2 ₁ 2 ₁	P2 ₁ 2 ₁ 2 ₁
unit cell dimensions <i>a</i> , <i>b</i> , <i>c</i> [Å]	46.48, 71.10, 101.05	46.71, 71.29, 100.92
resolution shell [Å]	41.0–1.40	1.43–1.40
total number of reflections	293 826	10 334
number of unique reflections	66 426	3106
completeness [%]	99.4	89.1
average <i>I</i> / σ (<i>I</i>)	22.6	4.6
<i>R</i> _{merge} [%] ^[a]	5.1	25.1
<i>R</i> _{meas} [%] ^[41]	5.7	30.2
<i>R</i> _{pim} [%] ^[42]	2.5	16.4
<i>R</i> _{cryst} [%] ^[b]		16.2
<i>R</i> _{free} [%] ^[c]		18.3
RMS deviation ^[d]	0.022 Å (2.0°)	0.024 Å (2.3°)
average <i>B</i> factors [Å ²] ^[e]	13.2, 16.1, 23.1, 23.9	11.5, 14.1, 17.2, 21.0
number of water molecules	273	259

[a] $R_{\text{merge}} = \frac{\sum_j \sum_h |I_{hj} - \langle I_h \rangle|}{\sum_j \sum_h \langle I_h \rangle} \times 100$.
 [b] $R_{\text{cryst}} = \frac{\sum |F_{\text{obs}}| - |F_{\text{calcd}}|}{\sum |F_{\text{obs}}|} \times 100$.
 [c] *R*_{free} = based on 5% of the total reflections. [d] RMS deviation from ideal for bonds (followed by the value for angles). [e] Average *B* factors in order: main chain, side chain, substrate and iron, solvent (water).

is pentacoordinate, bound by the side chains of His214, Asp216, His270, the homocysteiny l thiolate group and the water ligand opposite His214, and the valinyl isopropyl group sits in the binding site *trans* to Asp 216. In conformation B, the homocysteiny l carbonyl group is rotated approximately 60° “back” towards Phe211 (“back” relative to conformation A), taking up the position of the cysteinyl-derived carbonyl group in the IPNS:Fe^{II}:IPN and exposed IPNS:Fe^{II}:ACmC complexes.^[10] In those complexes the observed carbonyl rotation is the result of oxidative cyclisation (i.e., β -lactam formation), which cannot have occurred in the anaerobic IPNS:Fe^{II}:AhCV complex; we propose instead that carbonyl rotation in the AhCV complex reflects the conformational freedom of this region of the substrate. Rotation of the homocysteiny l carbonyl towards Phe211 moves the valinyl isopropyl group away from the iron binding site opposite Asp216. This allows a water ligand to coordinate iron in that position, and iron is hexacoordinate. As a result, the valinyl isopropyl is rotated approximately 30° relative to conformation A, occupying a position analogous to that observed in the IPNS:Fe^{II}:ACV:NO complex^[9] and IPNS:Fe^{II}:thiocarboxylate complex derived from δ -(L- α -aminoadipoyl)-L-cysteinyl D- α -hydroxyisovaleryl ester (ACOV).^[22]

Relative to ACV (1), AhCV (4) includes an additional methylene unit between C α and the side-chain thiol of its second residue. IPNS can accommodate this change, and binds AhCV well enough. However the price is greater conformational freedom for the enzyme-bound substrate, and some compromising of the tripeptide’s ability to reserve the iron-binding site opposite Asp216 for the cosubstrate oxygen to bind. Distortion at the homocysteiny l residue is translated along the substrate backbone, and affects conformation of both the amino-

dipoyl and valinyl regions as well. The conformational freedom is also translated to the protein itself, in the eight residues at the protein C terminus (Leu324–Thr331): regions of all these residues are poorly defined in the electron density map, indicating multiple occupancy/conformational freedom. Mobility in the C terminus has been linked to substrate binding and product departure from the IPNS active site.^[23] In the IPNS:Fe^{II}:AhCV complex it appears that the conformational changes required to accommodate the additional methylene group in the vicinity of the side chain of Leu324 destabilise the conformation of the whole protein tail relative to other anaerobic IPNS–substrate complexes.

The structure of the anaerobic IPNS:Fe^{II}:AhCmC complex

The thioether analogue AhCmC (12) was conceived so as to reduce some of the conformational freedom seen with AhCV (4). It was envisaged that coordination of the S-methylcysteinyl sulfur to iron would provide an extra anchor relative to AhCV (4) because thioether ligation to iron in the IPNS active site is well precedented.^[10,25,32,33]

The crystal structure of the IPNS:Fe^{II}:AhCmC complex was solved to 1.45 Å (Figure 2, Table 1). As in the case of the AhCV complex, the overall structure of the protein is well defined, and mirrors other IPNS–tripeptide complexes.^[9,16–18,30,31] Iron is bound by the His214, Asp216 and His270 side chains, a water ligand opposite His214 and the homocysteiny l thiolate.

The analogue AhCmC (12) is indeed better defined in the electron density map than AhCV (4), as anticipated. AhCmC (12) occupies the active site in two conformations in a 1:1 ratio, discussed below as conformation A [similar to the ACV-like conformation A seen with AhCV (4)] and conformation C (different from either of the principal conformations occupied by 4). In both conformations the substrate is tethered in the active site by enzyme–substrate interactions similar to those previously observed with ACV and other substrate analogues: through the thiolate sulfur to iron, through a salt bridge to the aminoadipoyl amino group, and with hydrogen bonds to the carboxylate group of the third residue (S-methylcysteine).^[9,22] In addition, the S-methylcysteinyl sulfur also coordinates to iron, as expected. The thioether sulfur sits 2.63 Å from the metal, a distance similar to those seen previously with δ -(L- α -aminoadipoyl)-L-cysteinyl-D-S-methylcysteine (ACmC, 2.69 Å),^[10] δ -(L- α -aminoadipoyl)-L-cysteinyl-D-thioisoleucine (ACTI, 2.66 Å)^[32] and δ -(L- α -aminoadipoyl)-L-cysteinyl-D-methionine (ACM, 2.57 Å).^[33] As a consequence the metal is hexacoordinate, in contrast to the IPNS:Fe^{II}:ACV and IPNS:Fe^{II}:AmCOV complexes^[9,22] and to conformation A of the IPNS:Fe^{II}:AhCV complex. This additional link between AhCmC (12) and the protein affixes this tripeptide much more rigidly in the IPNS active site than AhCV (4) and limits the conformational freedom otherwise imparted by the substitution of homocysteine for cysteine.

Conformation A of AhCmC (12, Figure 2) has a skeletal arrangement akin to those observed with ACV,^[9] ACOV^[22] and conformation A of AhCV (Figure 1). The S-methyl group is accommodated in the valinyl pocket with the methyl group

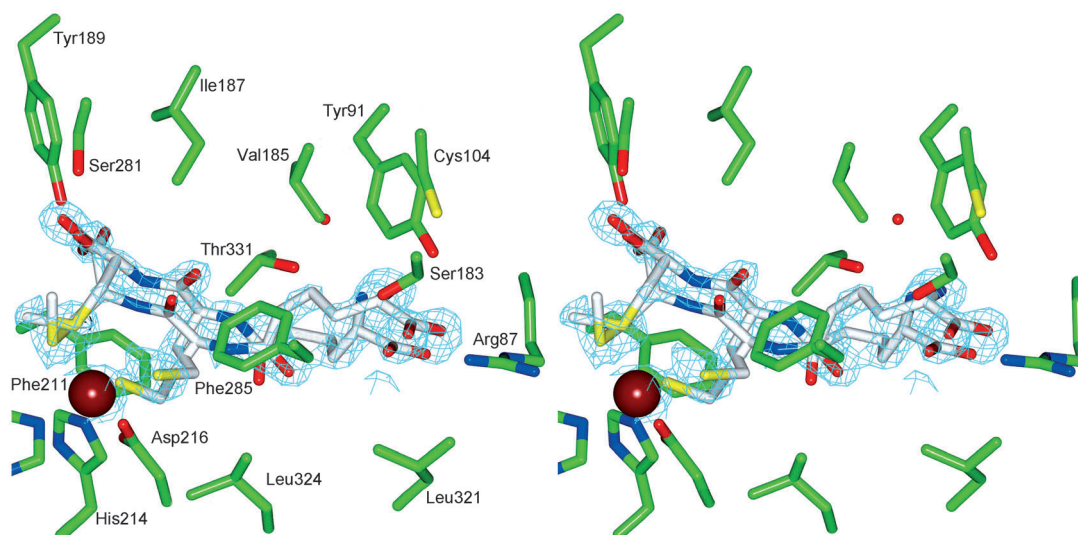


Figure 2. Stereoview of the active site of the IPNS:Fe^{II}:AhCmC complex, with electron density shown in cyan as $2mF_o - Df_c$ density^[43] at 1σ (where σ is the RMS value of the map over an asymmetric unit). The figure was generated by using CCP4mg.^[44]

pointing between the side chains of Leu231 and Leu223, as previously observed in the IPNS:Fe^{II}:ACmC complex.^[10] The γ -methylene group of the homocysteinyl residue sits “under” the homocysteinyl α -carbon in a position analogous to that of the cysteinyl β -carbon atom in the ACV complex; this forces the homocysteinyl β -carbon atom to sit “behind” the substrate backbone pointing towards Phe211.

In conformation C, the system finds alternative means to accommodate the additional methylene group of homocysteine. The *S*-methylcysteinyl residue has limited freedom to move, by virtue of the Fe–S(CH₃) linkage, so conformational change is forced on the amino adipoyl residue. Rotation about the C1–C α , C α –C β and C α –N bonds of homocysteine (hCys) bring the hCys C β towards Phe285 while maintaining its position “behind” the substrate backbone. This repositions the hCys C γ from “below” hCys C α to “below” the hCys N (“below” in the orientation shown in Figure 2). This change in the orientation of hCys C γ shunts the whole hCys–mCys portion of the tripeptide approximately 0.50 Å in the direction of the amino adipoyl carboxylate and Arg87. The amino adipoyl (L-AA) chain moves to accommodate these changes without compromising its links to the protein—in particular, the salt bridge to Arg87 is

preserved. The L-AA C β thus swings approximately 180° relative to conformation A, through rotation of the C γ –C δ bond towards Val185 and the C α –C β bond in an opposite sense. This reorganisation forces the C γ –C δ bond of the L-AA residue from a staggered to an eclipsed conformation (Figure 2).

The position of the *S*-methylcysteine residue is similar in both conformations, but the iron–sulfur distances for the thiolate and sulfide groups are significantly different in either case. The hCys thiolate group is 2.06 Å from iron in conformation A but 2.55 Å in conformation C; the mCys sulfide is 2.63 Å from the metal in conformation A, but only 2.41 Å away in conformation C. This reflects the overall shift in the position of the substrate towards Arg87 in conformation C relative to conformation A.

Conclusions

The crystal structures of the IPNS:Fe^{II}:AhCV and IPNS:Fe^{II}:AhCmC complexes evince the conformational flexibility of the second (homocysteinyl) residue in these substrates, relative to the shorter cysteinyl side chain in the native substrate ACV (1, Figure 3). The additional thioether tether to iron from

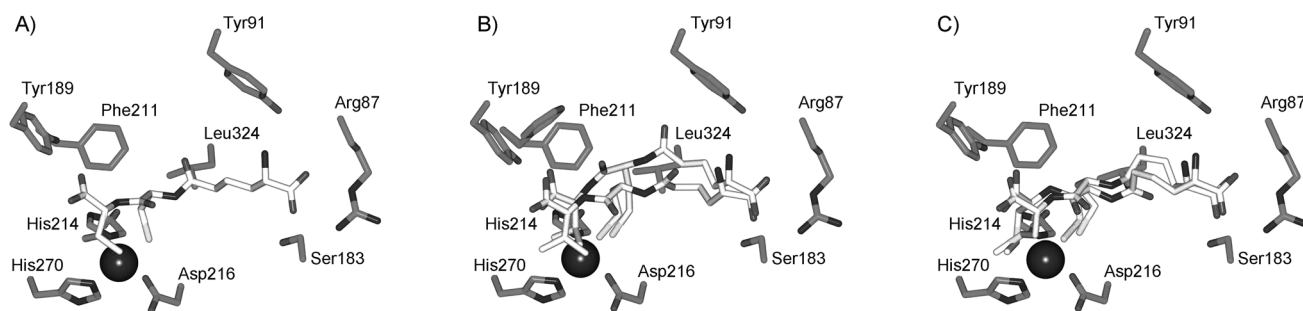


Figure 3. Comparison of substrate binding to iron in the complexes of IPNS with A) ACV (1, PDB ID: 1bk0), B) AhCV (4, PDB ID: 3zku), and C) AhCmC (12, PDB ID: 3zky). The figure was generated by using CCP4mg.^[44]

AhCmC (**12**) counteracts this flexibility to some extent, such that this substrate analogue occupies two distinct conformations. AhCV (**4**), without this additional anchor point, is even more mobile in the enzyme active site.

It is presumably this conformational fluidity that underpins the failure of monocyclic intermediate **6** to undergo the second ring closure (Scheme 2). We propose that the additional methylene group of the homocysteinyll residue forces subtle reorganisation of the active site such that the valinyl side chain is oriented away from the iron(IV)-oxo species in **6**. This would prevent reaction at valine C β (as occurs with ACV) and favour an alternative reaction pathway, leading to dissociation from the protein with loss of the homocysteinyll sulfur atom. Attempts to trap and to characterise intermediate **6** directly were unsuccessful: exposing crystals of either complex (IPNS:Fe^{II}:AhCV or IPNS:Fe^{II}:AhCmC) to high pressures of oxygen gas (20 bar) for various time periods (5 min to 24 h) returned only complex electron density maps that could not be resolved into coherent product structures (data not shown). Nonetheless, the crystal structures of the anaerobic IPNS:Fe^{II}:AhCV and IPNS:Fe^{II}:AhCmC complexes allow a better understanding of the reactions of IPNS with ACV analogues that incorporate homocysteine derivatives at the second position.

Experimental Section

Synthesis of tripeptide substrates

N-tert-Butoxycarbonyl- α -para-methoxybenzyl- δ -(*L*- α -aminoadipoyl)-*S*-para-methoxybenzyl-*L*-homocysteinyll-*D*-valine benzhydryl ester (**20**): Triethylamine (0.37 mL, 2.7 mmol) was added to a stirred solution of *N*-tert-butoxycarbonyl- α -para-methoxybenzyl- δ -(*L*- α -aminoadipoyl)-*S*-para-methoxybenzyl-*L*-homocysteine (**17**, 0.82 g, 1.3 mmol), *D*-valine benzhydryl ester *para*-toluenesulfonate salt (**18**, 0.61 g, 1.3 mmol), EDCI (0.26 g, 1.3 mmol) and HOBt (0.18 g, 1.3 mmol) in CH₂Cl₂ (20 mL). The reaction mixture was stirred for two days. After the stirring, further CH₂Cl₂ (20 mL) was added to the reaction mixture, which was then washed with water (20 mL), dilute HCl (1 M, 20 mL), and water again (20 mL). The CH₂Cl₂ solution was then concentrated in vacuo, and the residue was dissolved in ethyl acetate (20 mL). The solution was washed with saturated aqueous sodium bicarbonate (10 mL), water (10 mL), and saturated brine (10 mL), dried over magnesium sulfate and concentrated in vacuo. The crude product was purified by column chromatography (petroleum ether/ethyl acetate 80:20) to give **20** as a sticky white solid. Yield: 0.78 g (66%); m.p. 36–37 °C; *R*_f = 0.15 (CH₂Cl₂/ethyl acetate 90:10); [α]_D²⁴ = +3.05 (*c* = 0.53, CHCl₃); ¹H NMR (400 MHz, CDCl₃): δ = 0.77, 0.87 (2 d, *J* = 6.9 Hz, 6H; (CH₃)₂CH), 1.42 (s, 9H; (CH₃)₃C), 1.52–1.70 (m, 3H; 2 from NHCHCH₂CH₂CH₂, 1 from NHCHCH₂CH₂CH₂, 1.78–1.89 (2 overlapping m: m, 1H; 1 from NHCHCH₂CH₂CH₂; m, 1H; 1 from CHCH₂CH₂SCH₂Ar), 2.08–2.24 (3 overlapping m: m, 2H; 1 from CHCH₂CH₂SCH₂Ar and 1 from NHCHCH₂CH₂CH₂; m, 1H; 1 from NHCHCH₂CH₂CH₂; m, 1H; (CH₃)₂CH), 2.35–2.52 (m, 2H; CHCH₂CH₂SCH₂Ar), 3.67 (A of AB, *J*_{AB} = 14.5 Hz, 1H; 1 from SCH₂Ar), 3.70 (B of AB, *J*_{BA} = 14.0 Hz, 1H; 1 from SCH₂Ar), 3.78, 3.80 (2s, 6H; CH₃OArCH₂S and CH₃OArCH₂O), 4.22–4.35 (br m, 1H; NHCHCH₂CH₂CH₂), 4.60 (X of ABX, *J*_{XA} = 8.5 Hz, *J*_{XB} = 4.5 Hz, 1H; CHCH₂CH₂SCH₂Ar), 5.08 (A of AB, *J*_{AB} = 12.0 Hz, 1H; 1 from OCH₂Ar), 5.11 (B of AB, *J*_{BA} = 12.0 Hz, 1H; 1 from OCH₂Ar), 5.21 (d, *J* = 8.0 Hz, 1H; NHCHCH₂CH₂CH₂), 6.21 (d, *J* = 8.0 Hz, 1H; NHCHCH₂CH₂), 6.81 (d, *J* = 8.0 Hz, 1H; NHCHCH(CH₃)₂), 6.84 (d, *J*

8.5 Hz, 2H; 2CH_{Ar}), 6.88 (d, *J* = 9.0 Hz, 2H; 2CH_{Ar}) 7.22 (d, *J* = 8.5 Hz, 2H; 2CH_{Ar}), 7.26–7.41 ppm (12H; 12CH_{Ar}); ¹³C NMR (100.6 MHz, CDCl₃): δ = 17.2, 19.0, 21.2, 27.0, 28.2, 30.1, 31.8, 35.1, 35.3, 52.0, 52.9, 55.1, 55.2, 57.1, 66.8, 77.8, 79.8, 113.8, 126.8, 127.3, 127.4, 127.9, 128.1, 128.4, 129.8, 130.1, 139.3, 139.5, 155.4, 158.5, 159.6, 170.5, 171.0, 172.4, 172.6 ppm; IR (KBr disc): ν _{max} = 3302, 2964 (m), 1742, 1715, 1643, 1514, 1249, 1174 cm⁻¹; MS (APCI+): *m/z*: 884 (6) [M+H]⁺; HRMS: *m/z* calcd for C₄₉H₆₁N₃O₁₀SNa: 906.3975 [M+Na]⁺; found: 906.3947.

N-tert-Butoxycarbonyl- α -para-methoxybenzyl- δ -(*L*- α -aminoadipoyl)-*S*-para-methoxybenzyl-*L*-homocysteinyll-*S*-methyl-*D*-cysteine benzhydryl ester (**21**): Triethylamine (0.45 mL, 3.3 mmol) was added to a stirred solution of *N*-tert-butoxycarbonyl- α -para-methoxybenzyl- δ -(*L*- α -aminoadipoyl)-*S*-para-methoxybenzyl-*L*-homocysteine (**17**, 1.01 g, 1.6 mmol), *S*-methyl-*D*-cysteine benzhydryl ester *para*-toluenesulfonate salt (**19**, 0.77 g, 1.6 mmol), EDCI (0.31 g, 1.6 mmol) and HOBt (0.22 g, 1.6 mmol) in CH₂Cl₂ (20 mL). The reaction mixture was stirred at room temperature for two days. Further CH₂Cl₂ (20 mL) was then added, and the mixture was washed with water (20 mL), dilute HCl (1 M, 20 mL) and finally water (20 mL). The CH₂Cl₂ solution was concentrated in vacuo, and the residue was dissolved in ethyl acetate (20 mL). The ethyl acetate solution was washed with saturated aqueous sodium bicarbonate (10 mL), water (10 mL) and saturated brine (10 mL), dried over magnesium sulfate and concentrated in vacuo. The crude product was purified by column chromatography (petroleum ether/ethyl acetate 80:20) to give **21** as a sticky white solid. Yield: 0.68 g (46%); m.p. 73–74 °C; *R*_f = 0.15 (CH₂Cl₂/ethyl acetate 90:10); [α]_D²⁴ = +0.76 (*c* = 0.53, CHCl₃); ¹H NMR (500 MHz, CDCl₃): δ = 1.42 (s, 9H; (CH₃)₃C), 1.50–1.71 (m, 3H; 2 from NHCHCH₂CH₂CH₂, 1 from NHCHCH₂CH₂CH₂), 1.72–1.84 (m, 1H; 1 of NHCHCH₂CH₂CH₂), 1.85–1.97 (overlapping m and s: m, 1H; 1 from CHCH₂CH₂SCH₂Ar; s, 3H; CH₂SCH₃), 2.05–2.17 (3 overlapping m: m, 1H; 1 from CHCH₂CH₂SCH₂Ar; m, 1H; 1 from NHCHCH₂CH₂CH₂; m, 1H; 1 from NHCHCH₂CH₂CH₂), 2.39–2.52 (m, 2H; CHCH₂CH₂SCH₂Ar), 2.87 (A of ABX, *J*_{AB} = 14.0 Hz, *J*_{AX} = 6.5 Hz, 1H; 1 from CHCH₂SCH₃), 3.00 (B of ABX, *J*_{BA} = 14.0 Hz, *J*_{BX} = 5.0 Hz, 1H; 1 from CHCH₂SCH₃), 3.68 (s, 2H; SCH₂Ar), 3.78, 3.80 (2s, 6H; 3 from CH₃OArCH₂S and 3 from CH₃OArCH₂O), 4.23–4.33 (br m, 1H; NHCHCH₂CH₂CH₂), 4.58–4.67 (m, 1H; CHCH₂CH₂SCH₂Ar), 4.81–4.86 (m, X of ABX, 1H; CHCH₂SCH₃), 5.08 (A of AB, *J*_{AB} = 12.0 Hz, 1H; 1 from OCH₂Ar), 5.11 (B of AB, *J*_{BA} = 12.0 Hz, 1H; 1 from OCH₂Ar), 5.19 (d, *J* = 8.0 Hz, 1H; NHCHCH₂CH₂CH₂), 6.25 (d, *J* = 8.0 Hz, 1H; NHCHCH₂CH₂), 6.83 (d, *J* = 8.5 Hz, 2H; 2CH_{Ar}), 6.88 (d, *J* = 8.5 Hz, 2H; 2CH_{Ar}), 7.02 (d, *J* = 7.5 Hz, 1H; NHCHCH₂SCH₃), 7.22 (d, *J* = 8.5, 2H; 2CH_{Ar}), 7.26–7.41 ppm (m, 12H; 12CH_{Ar}); ¹³C NMR (125.7 MHz, CDCl₃): δ = 15.8, 21.2, 27.0, 28.2, 31.1, 31.8, 35.1, 35.2, 35.9, 51.6, 51.8, 52.9, 55.2, 66.8, 78.4, 79.8, 113.8, 127.0, 127.3, 128.1, 128.2, 128.5, 129.8, 129.9, 130.1, 139.0, 139.1, 155.4, 158.5, 159.6, 169.5, 170.8, 172.4 ppm; IR (KBr disc): ν _{max} = 3300, 2964, 1742, 1715, 1643, 1514, 1249, 1174 cm⁻¹; MS (APCI+): *m/z*: 902 (3) [M+H]⁺; HRMS: *m/z* calcd for C₄₈H₅₉N₃O₁₀S₂Na: 924.3540 [M+Na]⁺; found: 924.3533.

δ -(*L*- α -Aminoadipoyl)-*L*-homocysteinyll-*D*-valine (**4**): *N*-tert-Butoxycarbonyl- α -para-methoxybenzyl- δ -(*L*- α -aminoadipoyl)-*S*-para-methoxybenzyl-*L*-homocysteinyll-*D*-valine benzhydryl ester (**20**, 0.11 g, 0.12 mmol) was dissolved in TFA (5.0 mL). Anisole was added (0.60 mL, 5.5 mmol), and the reaction mixture was heated to reflux at 80–90 °C under argon with stirring. The reaction mixture was heated under reflux for 30 min and was then allowed to cool to room temperature, concentrated in vacuo and azeotroped with toluene (2 × 10 mL). The crude residue was dissolved in water (20 mL), and the resulting solution was washed with ethyl acetate (2 ×

10 mL). The combined organic phases were extracted with water (2 × 10 mL), and the pooled aqueous phases were back-extracted with ethyl acetate (10 mL). The combined aqueous extracts were lyophilised to give a yellow crusty solid. The crude product was purified by reversed-phase HPLC (C18, 250 × 10 mm; ammonium bicarbonate (10 mM in H₂O/MeOH) as eluent, running time: 0–6 min 0% MeOH, 6–13 min 25% MeOH, 13–20 min 0% MeOH; v/v, 4 mL min⁻¹) to yield **4** as a fluffy white solid. Yield: 12 mg (26%); *t*_R = 9 min 30 s; ¹H NMR (500 MHz, CDCl₃): δ = 0.77, 0.81 (2d, *J* = 7.0 Hz, 6H; (CH₂)₂CH), 1.52–1.69 (m, 2H; NHCHCH₂CH₂CH₂), 1.71–1.86 (m, 2H; NHCHCH₂CH₂CH₂), 1.95–2.01 (2 overlapping m: m, 2H; CHCH₂CH₂SH; m, 1H; (CH₃)₂CH), 2.25–2.35 (m, 2H; NHCHCH₂CH₂CH₂), 2.42–2.60 (m, 2H; CHCH₂CH₂SH), 3.65 (t, *J* = 6.0 Hz, 1H; NHCHCH₂CH₂CH₂), 4.01 (d, *J* = 6.0 Hz, 1H; (CH₃)₂CHCH), 4.48 ppm (X of ABX, *J*_{XA} = 9.0 Hz, *J*_{XB} = 5.5 Hz, 1H; CHCH₂CH₂SH); HRMS: *m/z* calcd for C₁₅H₂₆N₃O₆S: 376.1542 [*M*–H]⁻; found: 376.1538.

δ-(L-α-Amino adipoyl)-L-homocysteiny-D-S-methyl-cysteine (**12**): *N*-tert-Butoxycarbonyl-α-para-methoxybenzyl-δ-(L-α-amino adipoyl)-S-para-methoxybenzyl-L-homocysteiny-D-S-methyl-D-cysteine benzhydryl ester (**21**, 0.09 g, 0.10 mmol) was dissolved in TFA (4.0 mL). Anisole was added (0.50 mL, 4.6 mmol), and the reaction mixture was heated to reflux at 80–90 °C under argon with stirring. The mixture was heated at reflux for 30 min, and was then allowed to cool to room temperature, concentrated in vacuo and azeotroped with toluene (2 × 10 mL). The crude residue was dissolved in water (20 mL), and the aqueous solution was washed with ethyl acetate (2 × 10 mL). The combined organic phases were extracted with water (2 × 10 mL), and the pooled aqueous phases were back-extracted with ethyl acetate (10 mL). The combined aqueous extracts were lyophilised to give a yellow crusty solid. The crude product was purified by reversed-phase HPLC (see above) to yield **12** as a fluffy white solid. Yield: 4.8 mg (12%); *t*_R = 5 min 40 s; ¹H NMR (500 MHz, CDCl₃): δ = 1.52–1.70 (m, 2H; NHCHCH₂CH₂CH₂), 1.72–1.87 (m, 2H; NHCHCH₂CH₂CH₂), 1.90–2.05 (overlapping s and m: s, 3H; CH₂SCH₃; m, 2H; CHCH₂CH₂SH), 2.31 (t, *J* = 7.5 Hz, 2H; NHCHCH₂CH₂CH₂), 2.43–2.62 (m, 2H; CHCH₂CH₂SH), 2.75 (A of ABX, *J*_{AB} = 14.0 Hz, *J*_{AX} = 8.0 Hz, 1H; 1 from CH₂SMe), 2.93 (B of ABX, *J*_{BA} = 14.0 Hz, *J*_{BX} = 4.5 Hz, 1H; 1 from CH₂SMe), 3.65 (t, *J* = 6.0 Hz, 1H; NHCHCH₂CH₂CH₂), 4.29 (X of ABX, *J*_{XA} = 8.0 Hz, *J*_{XB} = 4.5 Hz, 1H; CHCH₂SMe), 4.48 ppm (X of ABX, *J*_{XA} = 9.5 Hz, *J*_{XB} = 5.0 Hz, 1H; CHCH₂CH₂SH); HRMS: *m/z* calcd for C₁₄H₂₄N₃O₆S₂: 394.1107 [*M*–H]⁻; found 394.1103.

Crystallography and structure determination: Crystals of the IPNS:Fe^{II}:AhCV and IPNS:Fe^{II}:AhCmC complexes were grown under anaerobic conditions as previously reported.^[34,35] Crystals suitable for X-ray diffraction were selected by use of a light microscope, removed from the anaerobic environment and exchanged into cryoprotectant buffer [a 1:1 mixture of well buffer and saturated lithium sulfate in glycerol (40%, v/v)], and were then flash-frozen in liquid nitrogen.

Data were collected at the European Synchrotron Radiation Source (ESRF), Grenoble, France, with use of an Oxford Cryosystems Cryostream and with the temperature maintained at 100 K. Data were processed with the aid of MOSFLM^[36] and the CCP4 suite of programs^[37] and then refined with REFMAC5^[38] and Coot for model building.^[39] Initial phases were generated by use of co-ordinates for the protein from the previously published IPNS:Fe^{II}:ACV structure,^[9] and manual rebuilding of protein side chains was performed as necessary. Crystallographic coordinates and structure factors have been deposited in the Worldwide Protein Data Bank, under

PDB ID: 3kzu (AhCV structure) and PDB ID: 3kzy (AhCmC structure). Figures 1 and 2 were prepared using CCP4mg.^[40]

Abbreviations

AC-: δ-(L-α-amino adipoyl)-L-cysteinyl-, ACmC: δ-(L-α-amino adipoyl)-L-cysteinyl-D-S-methylcysteine, ACOmC: δ-(L-α-amino adipoyl)-L-cysteinyl (1-(S)-carboxy-2-thiomethyl)ethyl ester, ACtI: δ-(L-α-amino adipoyl)-L-cysteinyl-D-thiaiso-leucine, ACV: δ-(L-α-amino adipoyl)-L-cysteinyl-D-valine, AhCV: δ-(L-α-amino adipoyl)-L-homocysteiny-D-valine, AhCaG: δ-(L-α-amino adipoyl)-L-homocysteiny-D-allylglycine, AhCmC: δ-(L-α-amino adipoyl) >-L-homocysteiny-D-S-methylcysteine, APCI: atmospheric pressure chemical ionisation, EDCl: 1-(3-dimethylaminopropyl)-3-ethylcarbodiimide hydrochloride, HOBt: 1-hydroxybenzotriazole hydrate, IPN: isopenicillin N, IPNS: isopenicillin N synthase, PMB: para-methoxybenzyl, TFA: trifluoroacetic acid.

Acknowledgements

We thank Dr. Nicolai Burzlaff, Dr. Jon Elkins, Professor Chris Schofield, and the scientists at the ESRF in Grenoble for help and discussions. Financial support was provided by the MRC, BBSRC and EPSRC.

Keywords: antibiotics • biosynthesis • enzyme mechanisms • lactams • metalloenzymes • non-heme iron enzymes

- [1] J. E. Baldwin, C. J. Schofield in *The Chemistry of β-Lactams* (Ed.: M. I. Page), Blackie, Glasgow, **1992**, pp. 1–78.
- [2] V. J. Chen, A. M. Orville, M. R. Harpel, C. A. Frolik, K. K. Surerus, E. Munck, J. D. Lipscomb, *J. Biol. Chem.* **1989**, *264*, 21677–21681.
- [3] R. A. Scott, S. Wang, M. K. Eidsness, A. Kriauciunas, C. A. Frolik, V. J. Chen, *Biochemistry* **1992**, *31*, 4596–4601.
- [4] C. R. Randall, L. Shu, Y.-M. Chiou, K. S. Hagen, M. Ito, N. Kitajima, R. J. Lachicotte, Y. Zang, L. Que, *Inorg. Chem.* **1995**, *34*, 1036–1039.
- [5] J. E. Baldwin, M. Bradley, *Chem. Rev.* **1990**, *90*, 1079–1088.
- [6] M. Wirstam, P. E. M. Siegbahn, *J. Am. Chem. Soc.* **2000**, *122*, 8539–8547.
- [7] M. Lundberg, P. E. M. Siegbahn, K. Morokuma, *Biochemistry* **2008**, *47*, 1031–1042.
- [8] P. L. Roach, I. J. Clifton, V. Fulop, K. Harlos, G. J. Barton, J. Hajdu, I. Andersson, C. J. Schofield, J. E. Baldwin, *Nature* **1995**, *375*, 700–704.
- [9] P. L. Roach, I. J. Clifton, C. M. H. Hensgens, N. Shibata, C. J. Schofield, J. Hadju, J. E. Baldwin, *Nature* **1997**, *387*, 827–830.
- [10] N. I. Burzlaff, P. J. Rutledge, I. J. Clifton, C. M. H. Hensgens, M. Pickford, R. M. Adlington, P. L. Roach, J. E. Baldwin, *Nature* **1999**, *401*, 721–724.
- [11] J. E. Baldwin in *Special Publication No. 52* (Eds.: A. G. Brown, S. M. Roberts), Royal Society of Chemistry, London, **1985**, pp. 62–85.
- [12] J. E. Baldwin, W. J. Norris, R. T. Freeman, M. Bradley, R. M. Adlington, S. Long-Fox, C. J. Schofield, *J. Chem. Soc. Chem. Commun.* **1988**, 1128–1130.
- [13] J. E. Baldwin, J. M. Blackburn, M. Sako, C. J. Schofield, *J. Chem. Soc. Chem. Commun.* **1989**, 970–972.
- [14] J. E. Baldwin, G. P. Lynch, C. J. Schofield, *J. Chem. Soc. Chem. Commun.* **1991**, 736–738.
- [15] A. C. Stewart, I. J. Clifton, R. M. Adlington, J. E. Baldwin, P. J. Rutledge, *ChemBioChem* **2007**, *8*, 2003–2007.
- [16] A. J. Long, I. J. Clifton, P. L. Roach, J. E. Baldwin, C. J. Schofield, P. J. Rutledge, *Biochem. J.* **2003**, *372*, 687–693.
- [17] A. R. Grummitt, P. J. Rutledge, I. J. Clifton, J. E. Baldwin, *Biochem. J.* **2004**, *382*, 659–666.
- [18] A. J. Long, I. J. Clifton, P. L. Roach, J. E. Baldwin, P. J. Rutledge, C. J. Schofield, *Biochemistry* **2005**, *44*, 6619–6628.

- [19] W. Ge, I. J. Clifton, J. E. Stok, R. M. Adlington, J. E. Baldwin, P. J. Rutledge, *Biochem. Biophys. Res. Commun.* **2010**, *398*, 659–664.
- [20] W. Ge, I. J. Clifton, J. E. Stok, R. M. Adlington, J. E. Baldwin, P. J. Rutledge, *Org. Biomol. Chem.* **2010**, *8*, 122–127.
- [21] A. Daruzzaman, I. J. Clifton, R. M. Adlington, J. E. Baldwin, P. J. Rutledge, *Arch. Biochem. Biophys.* **2013**, *530*, 48–53.
- [22] J. M. Ogle, I. J. Clifton, P. J. Rutledge, J. M. Elkins, N. I. Burzlaff, R. M. Adlington, P. L. Roach, J. E. Baldwin, *Chem. Biol.* **2001**, *8*, 1231–1237.
- [23] J. M. Elkins, P. J. Rutledge, N. I. Burzlaff, I. J. Clifton, R. M. Adlington, P. L. Roach, J. E. Baldwin, *Org. Biomol. Chem.* **2003**, *1*, 1455–1460.
- [24] A. Daruzzaman, I. J. Clifton, R. M. Adlington, J. E. Baldwin, P. J. Rutledge, *ChemBioChem* **2006**, *7*, 351–358.
- [25] W. Ge, I. J. Clifton, J. E. Stok, R. M. Adlington, J. E. Baldwin, P. J. Rutledge, *J. Am. Chem. Soc.* **2008**, *130*, 10096–10102.
- [26] W. Ge, I. J. Clifton, A. R. Howard-Jones, J. E. Stok, R. M. Adlington, J. E. Baldwin, P. J. Rutledge, *ChemBioChem* **2009**, *10*, 2025–2031.
- [27] V. du Vigneaud, H. M. Dyer, J. Harmon, *J. Biol. Chem.* **1933**, *101*, 719–726.
- [28] S. Wolfe, M. G. Jokinen, *Can. J. Chem.* **1979**, *57*, 1388–1396.
- [29] M. Bodanzky, A. Bodanzky in *Reactivity and Structure Concepts in Organic Chemistry, Vol. 21* (Eds.: K. Hafner, C. W. Rees, B. M. Trost, J. M. Lehn, P. v. R. Schleyer, R. Zahrachik), Springer, Berlin, **1984**, pp. 172–173.
- [30] A. R. Howard-Jones, P. J. Rutledge, I. J. Clifton, R. M. Adlington, J. E. Baldwin, *Biochem. Biophys. Res. Commun.* **2005**, *336*, 702–708.
- [31] A. R. Howard-Jones, J. M. Elkins, I. J. Clifton, P. L. Roach, R. M. Adlington, J. E. Baldwin, P. J. Rutledge, *Biochemistry* **2007**, *46*, 4755–4762.
- [32] I. J. Clifton, W. Ge, R. M. Adlington, J. E. Baldwin, P. J. Rutledge, *ChemBioChem* **2011**, *12*, 1881–1885.
- [33] I. J. Clifton, W. Ge, R. M. Adlington, J. E. Baldwin, P. J. Rutledge, *Arch. Biochem. Biophys.* **2011**, *516*, 103–107.
- [34] P. L. Roach, I. J. Clifton, C. M. H. Hensgens, N. Shibata, A. J. Long, R. W. Strange, S. S. Hasnain, C. J. Schofield, J. E. Baldwin, J. Hajdu, *Eur. J. Biochem.* **1996**, *242*, 736–740.
- [35] P. J. Rutledge, N. I. Burzlaff, J. M. Elkins, M. Pickford, J. E. Baldwin, P. L. Roach, *Anal. Biochem.* **2002**, *308*, 265–268.
- [36] A. G. W. Leslie, *Acta Crystallogr. Sect. D Biol. Crystallogr.* **1999**, *55*, 1696–1702.
- [37] Collaborative Computational Project Number 4, *Acta Crystallogr. Sect. D Biol. Crystallogr.* **1994**, *50*, 760–763.
- [38] G. N. Murshudov, A. A. Vagin, E. J. Dodson, *Acta Crystallogr. Sect. D Biol. Crystallogr.* **1997**, *53*, 240–255.
- [39] P. Emsley, K. Cowtan, *Acta Crystallogr. Sect. D Biol. Crystallogr.* **2004**, *60*, 2126–2132.
- [40] L. Potterton, S. McNicholas, E. Krissinel, J. Gruber, K. Cowtan, P. Emsley, G. N. Murshudov, S. Cohen, A. Perrakis, M. Noble, *Acta Crystallogr. Sect. D Biol. Crystallogr.* **2004**, *60*, 2288–2294.
- [41] K. Diederichs, P. A. Karplus, *Nat. Struct. Biol.* **1997**, *4*, 269–275.
- [42] M. S. Weiss, *J. Appl. Crystallogr.* **2001**, *34*, 130–135.
- [43] R. J. Read, *Acta Crystallogr. Sect. A Found. Crystallogr.* **1986**, *42*, 140–149.
- [44] S. McNicholas, E. Potterton, K. S. Wilson, M. E. M. Noble, *Acta Crystallogr. Sect. D Biol. Crystallogr.* **2011**, *67*, 386–394.

Received: November 21, 2012

Published online on March 7, 2013